1-1-2024

The use of variable coil pitch of helical tube on the hydro-thermal performance improvement

Shayan Pourhemmati
Edith Cowan University

Hussein A. Mohammed
Edith Cowan University

Abdellah Shafieian
Edith Cowan University

10.1016/j.csite.2023.103944
Pourhemmati, S., Mohammed, H. A., & Shafieian, A. (2024). The use of variable coil pitch of helical tube on the hydro-thermal performance improvement. Case Studies in Thermal Engineering, 53, article 103944. https://doi.org/10.1016/j.csite.2023.103944

Case Studies in Thermal Engineering 53 (2024) 103944

Contents lists available at ScienceDirect

Case Studies in Thermal Engineering

journal homepage: www.elsevier.com/locate/csite

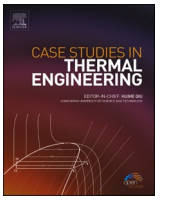

The use of variable coil pitch of helical tube on the hydro-thermal performance improvement

Shayan Pourhemmati, Hussein A. Mohammed *, Abdellah Shafieian

School of Engineering, Edith Cowan University, 270 Joondalup Drive, WA, 6027, Australia

HIGHLIGHTS

- The helical tube with variable pitch is introduced and compared with the conventional design.
- The modification of radial pitch leads to better overall performance enhancement.
- Thinning the thermal boundary layers is detected as the main reason for heat augmentation.

ARTICLE INFO

Handling Editor: Huihe Qiu

Keywords:
Helical tube
Thermal performance
Computational fluid dynamics
Laminar flow
Numerical study
Pressure-drop
Dean vortices

ABSTRACT

The use of helical tubes in heat transfer appliances is desirable due to their better heat transfer characteristics, but the higher pressure drop decreases the overall performance. The variation of pitch design of a helical tube is proposed to alleviate this situation so that the pitch number does not remain constant in the total tube length. A total of six variable pitch numbers with three different diameters are proposed and investigated on the thermal and fluid characteristics. To better understand the helical tube efficiency, PEC (performance evaluation criteria) is selected as a performance indicator in the present work and simulations are performed in a laminar regime ($100 \leq Re \leq 1600$) at a constant heat flux boundary condition using computational fluid dynamics. The numerical results show that variable radial pitch has higher effects on the overall performance than variable axial pitch, and it can intensify the helical tube performance by up to 10%. The results also indicate that increasing the tube diameter leads to heat transfer and friction factor increment while increasing the Reynolds number deteriorates the overall performance.

Nomenclature

A	area of cross-section (m^2)
q	conductive flux ($W \bullet m^{-2}$)
δ	curvature ratio
u	fluid velocity (m/s)
Q	heat rate (W)
R	helical coil radius (cm)
r	inner radius of helical tube (cm)
j	absolute vorticity flux along the normal direction of cross section (1/s)

* Corresponding author.
E-mail addresses: spourhem@our.ecu.edu.au (S. Pourhemmati), hussein.mohammed@ecu.edu.au (H.A. Mohammed), a.shafieiandastjerdi@ecu.edu.au (A. Shafieian).

https://doi.org/10.1016/j.csite.2023.103944
Received 14 September 2023; Received in revised form 31 October 2023; Accepted 22 December 2023
Available online 30 December 2023

$\dot{m}$	mass flow rate (kg•s^{-1})
p	pressure (kPa)
P	pitch of helical tube (cm)
C_p	specific heat capacity (J•Kg^{-1}•K^{-1})
k	thermal conductivity (W•m^{-1}•K^{-1})
T	temperature (K)
H	variable pitch step (cm)
D	winding diameter (cm)

Abbreviations

Dn	Dean number
HTF	heat transfer fluid
Nu	Nusselt number
Pr	Prandtl number
str	straight tube

Greek symbols

ρ	density (kg•m^{-3})
ω	vorticity (1s•$^{-1}$)
μ	fluid dynamic viscosity (Pa•s)

Subscripts

a	axial
aw	average weighted
ave	average
f	fluid
i	inner
in	inlet
o	outer
out	outlet
r	radial
s	solid
w	wall

1. Introduction

Heat transfer improvement with minimum pressure drop in heat exchangers is the primary goal of thermal engineering. Many types of heat exchangers have been introduced for different applications by considering the thermal capacity, weight and size. Consequently, various techniques are taken to improve their overall performance [1]. Generally, two approaches are considered for heat transfer augmentation: passive technique and active technique. In the first one, there is no need for external power to increase the heat transfer, while in the second method, the external power source is implemented in the thermal devices to raise the heat transfer rate. Among tube exchangers, the helical tube heat exchanger has unique features which give particular potential in some applications. It is widely used in power conversion systems, chemical processing, thermal power plants, nuclear reactors, solar energy concentrator receivers, medical equipment, and waste heat recovery systems [2,3]. A helical tube provides a specific fluid pattern for heat transfer fluid (HTF), compactness, and low manufacturing cost. They outperform straight tubes because they create vorticity in the main fluid flow, which increases the heat transfer rate by destroying and restarting boundary layers. Vorticity is created because of the pressure difference between the inner and outer tubes' curvatures during the fluid turn.

The double micro helical tube is assessed by Abu-Hamdeh et al. [4]. The length of tubes by adjusting the turn number is kept constant for all considered configurations. Overall, 12 cases with different pitch numbers were proposed, and they found that the overall trend of performance indicators decreased by increasing the coil pitch number. Wu et al. [5] investigated the three-groove configurations on the helical tube, namely the helical transverse-groove tube, helical grooved tube, and helical longitudinal-groove tube in the turbulent regime. After the first investigation, they comprehend that helical longitudinal grooves with semi-circular shapes outperform other designs. So, they adopted an optimization for this geometry in terms of groove depth, groove number, and groove angle. The result showed that the overall performance indicator is more sensitive to groove angle than other parameters. The impact of circular depressions on thermal performance in the double-tube helical heat exchanger was analyzed by Cao et al. [6]. They confirmed that inner tube depressions have better overall performance than other models in turbulent regimes ($10000 \leq Re \leq 14000$). The incorporation of fins in the micro helically coiled tube was numerically investigated in a turbulent regime by Kumar [7]. Three fin numbers were investigated for cases; 4, 8 and 12, and the deduced result indicates that 12 fins can improve the overall performance more than others. They pointed out that a small coil diameter and pitch contribute to overall improvement in the performance of the helical tube. Zheng [8] investigated the helical semi-circular groove on the helical tube. Various geometrical parameters like

corrugation depth and corrugation pitch were considered. They confirmed that increasing corrugation pitch leads to the decrease of Nusselt number and friction factor and increasing depth results in growing trends in these dimensionless numbers. Helical tube with rib configuration was introduced by Hasan et al. [9]. The rib number and its revolution in the helical tube are considered. Low-head and high-rib revolutions showed better heat transfer characteristics for helical tube heat exchangers. In a numerical study by Chen et al. [10], the corrugated helical tube was investigated under the turbulent regime. Their findings denote the PEC number falls between 0.63 and 1.01 for investigated cases, and decreasing the corrugation height and pitch leads to an increase in this number. They also understood that corrugated tubes have a lower total cost per unit transferred heat load, up to 9%. Kirkar et al. [11] investigated the helical tube heat exchanger with corrugated walls. They confirmed that a smaller helical coil diameter leads to better results in terms of hydraulic and thermal performance, and overall performance is considerably high compared to the smooth straight tube in a laminar regime, while the overall efficiency indicator drops significantly due to a high-pressure drop in the turbulent flow regime.

Tape insertion is a common method in straight tubes for heat transfer improvement, and this technique is extensively investigated by introducing various shapes and designs. Some researchers extended this method to helical tubes and examined its efficiency. Liaw et al. [12] analyzed the effect of the insertion of twisted tape in a helical tube for Reynolds number between 10000 and 20000. Under constant wall temperature, they prove the high overall performance of helical tubes with simple twisted tape against straight tubes with tape. However, considerable pressure drop in the helical tube with tape insertion hinders it from outperforming a helical tube without tape. In a similar study [13], the insertion of simple twisted tape in a helical tube is investigated in a laminar regime ($100 \leq Re \leq 2000$) for low Pr number (air) and high *Pr* number (water). The result confirms that the helical tube without twisted tape performs better than the straight tube without and with twisted tape in low Reynolds numbers for both HTF. They noticed that the insertion of twisted tape in a helical tube does not improve the overall heat transfer compared to no tape condition and even hinders it from outperforming a straight tube without tape. In another study, twisted tape insertion for a turbulent regime was experimentally investigated by Xie et al. [14]. Their results did not show significant improvement of the helical tube performance, and the maximum PEC = 1.01 is registered for the lowest pitch at the lowest Reynolds number. A significant pressure drop by insertion of the coil in the helical tube was observed by Ehsan Gholamalizadeh et al. [15]. They analyzed the unconventional inserts such as S-profile, concentric circle, eccentric circle, and two rectangular and square shapes in a helical tube and concluded that square and two rectangular profiles have the most effect on raising the heat transfer rate and pressure drop in both flow regimes. Their investigation indicated that the two rectangular and eccentric circles are the best candidates in the laminar and turbulent flow, respectively.

A multi-tube in-tube helical coil is investigated by Fouda et al. [16]. Several geometrical parameters were taken into consideration in their work. The obtained result shows that helical coil pitch has a negligible effect on the overall performance, while the helical coil's diameter significantly affects the overall efficiency. The impact of implementing tubes inside the helical tube shows that the overall performance increases up to three tubes and then decreases to five tubes. A similar study is conducted by Elattar et al. [17] who investigated the insertion of multi-tube in tube helical coil and confirmed that increasing the number of tubes up to 3 has a positive effect on the heat exchanger effectiveness, but it leads to adverse outcomes for numbers 4 and 5. Helical multilobe tubes were considered in the work of Liaw et al. work [18]. The result denoted that increasing the number of lobes cannot significantly improve the heat transfer rate, and twisting these helical tubes adversely affects the overall heat transfer coefficient. Another study [19] investigated multi-tube thermal-hydrodynamic performance in helical coiled tube heat exchangers. They concluded that decreasing the coil diameter or increasing the coiled pitch can improve hydro-thermal performance. Wang et al. [20] explored the three new types of helical tubes inside the shell and tube heat exchanger and compared them with the helically coiled plain tube. The findings indicated that the helically coiled-twisted trilobal tube has better performance in comparison with the helically coiled elliptical tube and helically coiled trilobal tube. However, the overall performance indicators are close together, and significant performance discrepancy is only found when these new helical tubes are compared with helically coiled plain tubes.

The twisted tube would be an interesting option for heat transfer augmentation, and some of the studies with this method are summarised in the following section. In a numerical analysis done by Halawa and Tanious [21] who considered the twisted and non-twisted helical tubes with various elliptical cross sections. They showed that widening cross-section in the helical tube's radial direction positively affects the Nusselt number because of the increased turbulent kinetic energy in circumferences. The pitch ratio analyses show non-linear behaviour; however, for higher pitch ratios, the overall performance is higher than the lower ones. Chang et al. [22] introduced a square cross-section helical tube. Four twisted patterns were compared with a non-twisted configuration, and the result indicated that the smaller twisted pitches increase the pressure drop and heat transfer simultaneously. However, this augmentation does not lead to outperforming the overall performance of the non-twisted pattern. In a similar study, the helical tube with twisted and non-twisted square cross-sections is investigated experimentally and numerically by Farnam et al. [23]. They confirmed that helical pitch has negligible impact on the performance while helical coil diameter and twist pitch can significantly impact the pressure drop and heat transfer rate. In the numerical investigation of Luo et al. [24] who studied an aero engine's double helically coiled heat exchanger. They considered eight eccentric angles and five eccentric ratios of the inner tube. In other words, they embed the inner tube in different directions and locations in order to comprehend the fluid flow and heat transfer pattern. Several numerical simulations for the turbulent regime were also taken, and the results indicated that the overall performance increased by up to 14% compared to the typical tube in tube helical coil. They found that the eccentric angle does not significantly affect the heat transfer improvement as much as the eccentric ratio. Another similar study in the field of air engines was done by Muyi Fan et al. [25]. They analyzed the flow and heat transfer in the eccentric annulus of the double-helical heat exchanger. The result confirmed that the fluid flow in the annulus becomes complicated and chaotic for positive eccentric ratios (inner tube near to outer side). The higher Nusselt numbers of annulus fluid appeared by increasing the eccentric ratios, while the highest friction factor was observed in the centric position of the inner tube. For the inner tube, the negligible friction and Nusselt number variation were observed by variation of eccentric ratio.

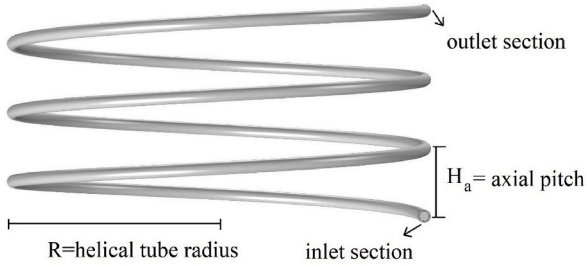

Fig. 1. The schematic of the conventional helical tube.

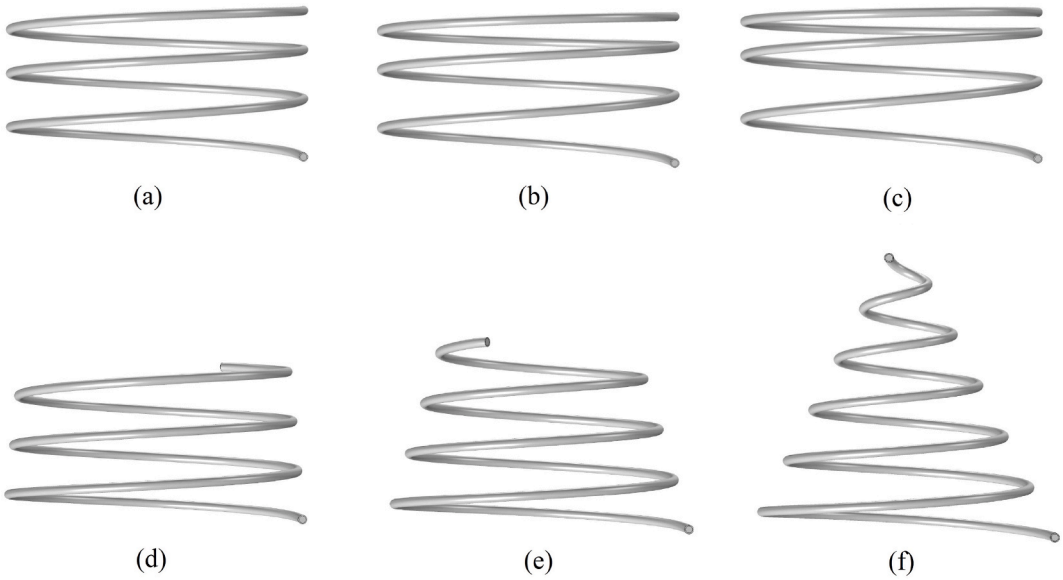

Fig. 2. The schematic of new designs (a–c) variable axial pitch with step size of ($H_a = 1$, $H_a = 2$ and $H_a = 3$ cm), and (d–f) variable radial pitch with step size of ($H_r = 0.5$, $H_r = 1$ and $H_r = 2.5$ cm).

From previous studies, it can be inferred that the pressure drops in helical tubes significantly impact the overall performance, and some techniques, like tape insertion, do not lead to significant improvement. Also, the effect of constant coil pitch has been widely investigated, and most studies considered the helical tube in turbulent working conditions. The current study aims to investigate variable pitch effects in a helical tube for laminar fluid flow. For this, two pitch patterns in axial and radial directions are proposed, and all considered cases are studied under identical tube lengths to make a fair comparison. The Dean number would be suitable for predicting heat transfer augmentation but does not consider pressure penalty. So, relying on this number would be misleading, and PEC is selected for overall performance evaluation in the current study. Along with variable pitch designs, the effect of tube diameter is also considered, and thermal and velocity contours for a better understanding of the fluid flow pattern and heat transfer are provided in identical Reynolds numbers.

2. Modelling methodology

2.1. Physical model

The 3-D view of the basic helical tube on the X-Z plane is presented in Fig. 1. The basic model of a helical tube consists of three turns and is made of copper. The axial coil pitch, helical coil radius, inner diameter, and tube thickness are 5 cm, 15 cm, 0.7 cm, and 0.1 cm, respectively. The length of the helical tube is 283 cm, and its height in the Z direction is equal to 15 cm. The pitch number in the conventional model does not change. However, the variable design offers a changeable pitch along the axial and radial directions. In all considered models, the fluid flows from the bottom of the helical coil and exits from the top side, and the tube wall thickness does not change. The schematics of the variable axial pitch are presented in Fig. 2(a–c). The three pitch steps ($H_a = 1$, 2, and 3 cm) in the axial direction are considered in the current study, and their effect on heat and fluid flow behaviour is analyzed. For this structural design, the relative axial pitch changes along the axial direction while the absolute axial pitch remains constant. In other words, the total length of the tube remains equal to the conventional helical tube. For a helical tube with step size $H_a = 3$ cm, the axial pitch decreases by 3 cm from the inlet to the outlet section for every turn. Thus, the first, second, and third axial pitch is selected as 8, 5, and 2 cm,

Table 1
The geometrical parameters details of helical tubes.

Case	axial pitch	helical tube radius	variable axial pitch (H_a)	variable radial pitch (H_r)	number of tube turns	tube length
$H_a = 1$	–	15 cm	1 cm	0 cm	3	283 cm
$H_a = 2$	–	15 cm	2 cm	0 cm	3	283 cm
$H_a = 3$	–	15 cm	3 cm	0 cm	3	283 cm
$H_r = 0.5$	5 cm	–	0 cm	0.5 cm	3.16	283 cm
$H_r = 1.5$	5 cm	–	0 cm	1 cm	3.66	283 cm
$H_r = 2.5$	5 cm	–	0 cm	2.5 cm	5.49	283 cm
Conventional	5 cm	15 cm	0 cm	0 cm	3	283 cm

Table 2
The thermophysical properties of copper.

Materials	Density (kg/m^3)	Thermal conductivity (W/m.K)	Heat capacity (J/kg.K)	Dynamic viscosity (Pa.s)
Copper	8960	400	385	–

respectively. Fig. 2(d–f) illustrates the helical tube with variable radial pitch (tapered design), in which the helical coil pitch step varies along the radius direction. Similar to the previous model, the tube's total length remains unchanged compared to the basic model, while to make the tube length equal to the conventional model, the number of tube turns increased for this model. The three pitch steps in the radial direction ($H_r = 0.5$, 1.5, and 2.5 cm) are proposed for this model. The configuration with $H_r = 2.5$ cm is shown in Fig. 2(f), which denotes that the helical coil radius pitch decreases by 2.5 cm in every 360-degree turn. The details of the geometrical parameters of helical tubes are presented in Table 1. It is necessary to mention that the radial pitch is zero for conventional and variable axial pitch designs, as the helical coil radius does not change. The thermophysical properties of copper are provided in Table 2, while the temperature-dependent properties are considered for water to increase accuracy. These properties are supplied in Eqs. (1)–(4) [26–29].

$$\mu(T) = 1.3799566804 - 0.021224019151 \bullet T + 1.3604562827 \bullet 10^{-4} \bullet T^2 - 4.6454090319 \bullet 10^{-7} \bullet T^3 + 8.9042735735 \bullet 10^{-10} \bullet T^4 - 9.0790692686 \bullet 10^{-13} \bullet T^5 + 3.8457331488 \bullet 10^{-16} \bullet T^6 \quad (1)$$

$$C_p(T) = 12010.1471 - 80.4072879 \bullet T + 0.309866854 \bullet T^2 - 5.38186884 \bullet 10^{-4} \bullet T^3 + 3.62536437 \bullet 10^{-7} \bullet T^4 \quad (2)$$

$$\rho(T) = 0.000010335053319 \bullet T^3 - 0.013395065634452 \bullet T^2 + 4.969288832655160 \bullet T + 432.257114008512 \quad (3)$$

$$k(T) = -0.869083936 + 0.00894880345 \bullet T - 1.58366345 \bullet 10^{-5} \bullet T^2 + 7.97543259 \bullet 10^{-9} \bullet T^3 \quad (4)$$

2.2. Governing equations and boundary conditions

For studying conjugate heat transfer between solid and fluid domains, finite element method was used with the following assumptions:

- The flow is steady and incompressible.
- The fluid properties are dependent on temperature.
- Fluid is considered incompressible and fully developed laminar flow.
- Viscous dissipation, gravitational force, radiative heat transfer and surface roughness are ignored.

Based on the above assumptions, continuity, momentum, and energy equations are described in Eqs. (5)–(8) [30]. In the above equations: ρ_f, u, p, k, μ, T and C_p are defined as the fluid density, fluid velocity, pressure, thermal conductivity, viscosity of fluid, temperature and specific heat capacity, respectively.

$$\nabla.(\rho_f u) = 0 \quad (5)$$

$$u.\nabla.(\rho_f u) = -\nabla p + \nabla.(\mu \nabla u) \quad (6)$$

$$u.\nabla(\rho_f C_p k_f) = \nabla.(k_f \nabla T_f) \quad (7)$$

$$\nabla(k_s \nabla T) = 0 \quad (8)$$

The boundary conditions are presented as follows:

(continued on next page)

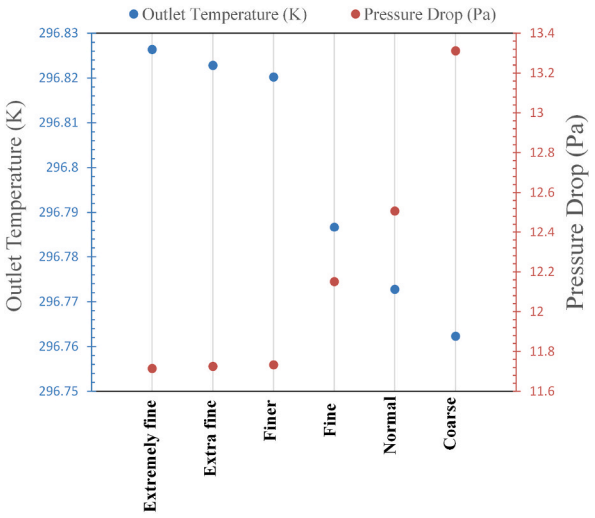

Fig. 3. Grid independency investigation.

(*continued*)

At the inlet area of the channel: $T = T_{in} = 293.15$ K, $u = u_{m,f}$, $v = w = 0$	(9)
In the above equation, u, v and w are the velocity components in the X, Y and Z directions, respectively. Where $u_{m,f}$ is defined as the mean inlet velocity of fluid	
At the outlet area of channel: $P = P_{atm} = 1$ atm	(10)
At the contact surface of solid and working fluid, no slip condition is considered: $U = 0$, $V = 0$, $W = 0$	(11)
At the outer surface of the helical tube: $z = 0$, $q_w = -k_s \frac{\partial Ts}{\partial n} = 400 \frac{W}{m^2}$	(12)

2.3. Performance analysis

The Reynolds number, friction coefficient, Nusselt number, heat transfer coefficient and PEC number are mentioned in Eq. (13)–(18) [31], respectively. In the these equations; D_h, Δp, $u_{m,f}$, $T_{w,ave}$, $T_{f,ave}$ and L_x are the hydraulic diameter, the absolute pressure difference between inlet and outlet, the mean velocity of HTF, the average temperature of walls, the average temperature of HTF and the total length of the tube, respectively. As mentioned before, PEC (performance evaluation criteria) is selected as a performance indicator to evaluate the thermal-hydraulic characteristics of the helical tube. This indicator is calculated at a constant Reynolds number for all cases in this paper, and Nu_0 and f_0 refer to the conventional helical tube.

$$Re = \frac{\rho\, U_{m,f}\, D_h}{\mu} \tag{13}$$

$$f = \frac{2 D_h\, \Delta p}{\rho\, L_x\, {U_{m,f}}^2} \tag{14}$$

$$Nu_{ave} = \frac{h^{-}_{ave}\, D_h}{K_f} \tag{15}$$

$$h^{-}_{ave} = \frac{q_w}{(T_{w,ave} - T_{f,ave})} \tag{16}$$

$$T_{f,ave} = \frac{T_{out,aw} - T_{in,aw}}{2} \tag{17}$$

$$PEC = \frac{\frac{Nu}{Nu_0}}{\left(\frac{f}{f_0}\right)^{1/3}} \tag{18}$$

The generation of vortex flow inside the helical tube was reported in the previous studies. In order to better comprehend this parameter in the quantitative form, the magnitude of this is computed and compared to other models by Eqs. (19) and (20) [32,33]. The vorticity magnitude is described by the absolute vorticity flux in the normal direction of the cross-section and can be written as follows:

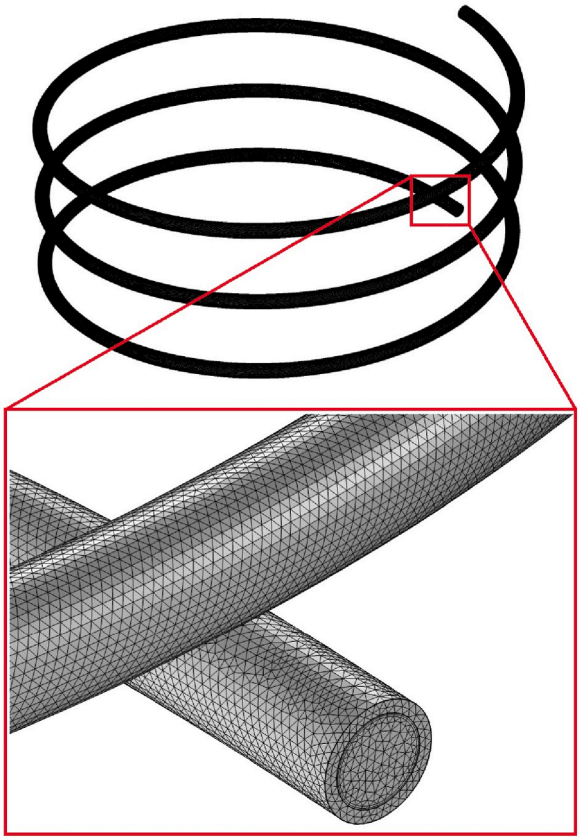

Fig. 4. The detail of mesh for extra fine layout.

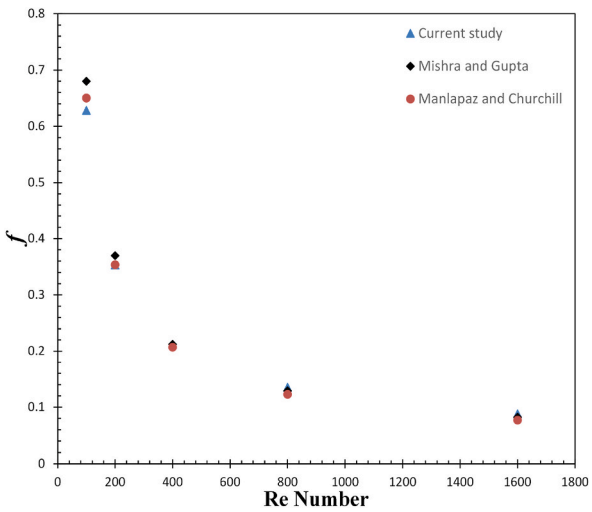

Fig. 5. Comparison of Mishra and Gupta [34], Manlapaz and Churchill [35] correlations with the present work.

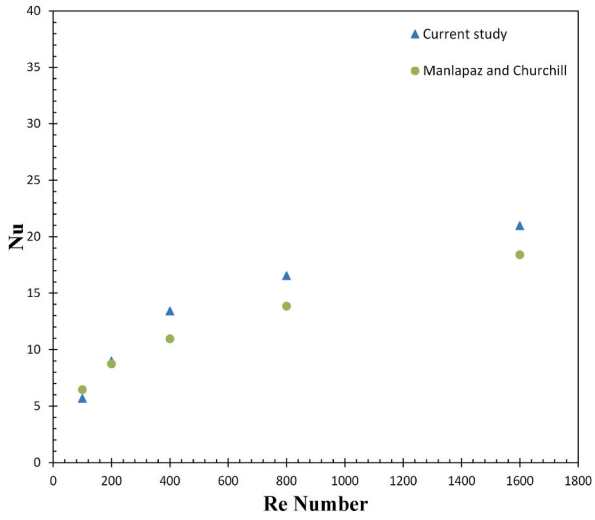

Fig. 6. Comparison of Manlapaz and Churchill [36] correlation with the present work.

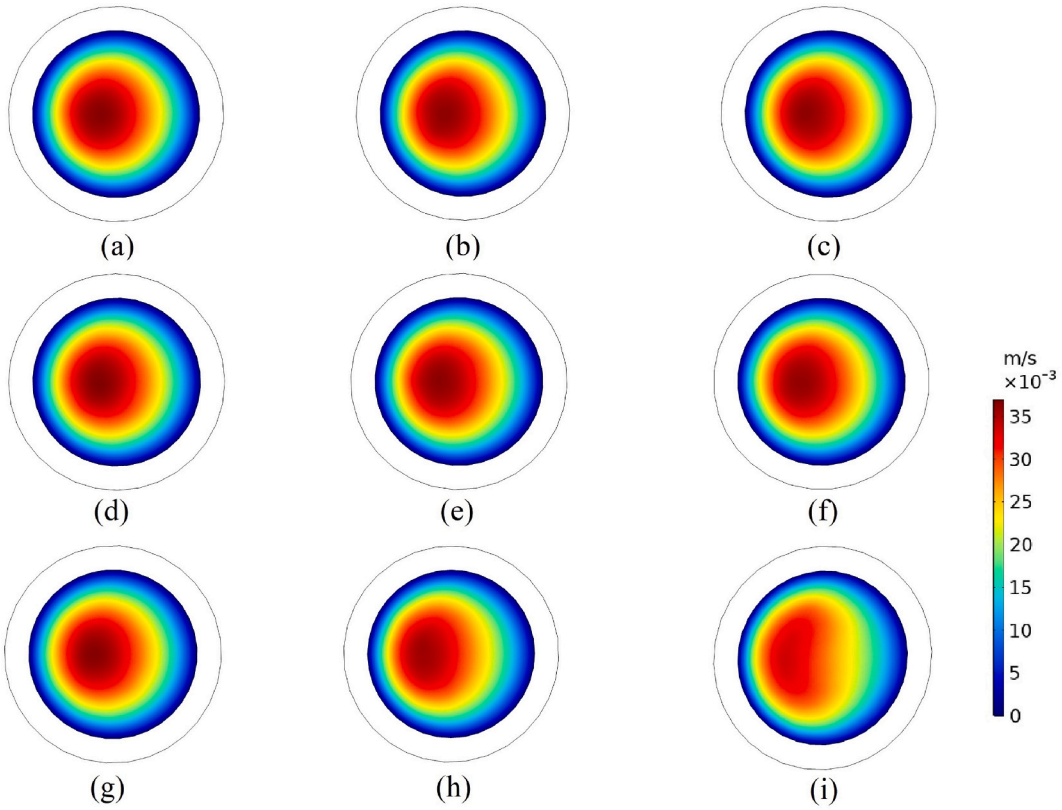

Fig. 7. The velocity distribution (a–c) conventional helical tube, (d–f) variable axial pitch (H_a = 3 cm), and (g–i) variable radial pitch (H_r = 2.5 cm).

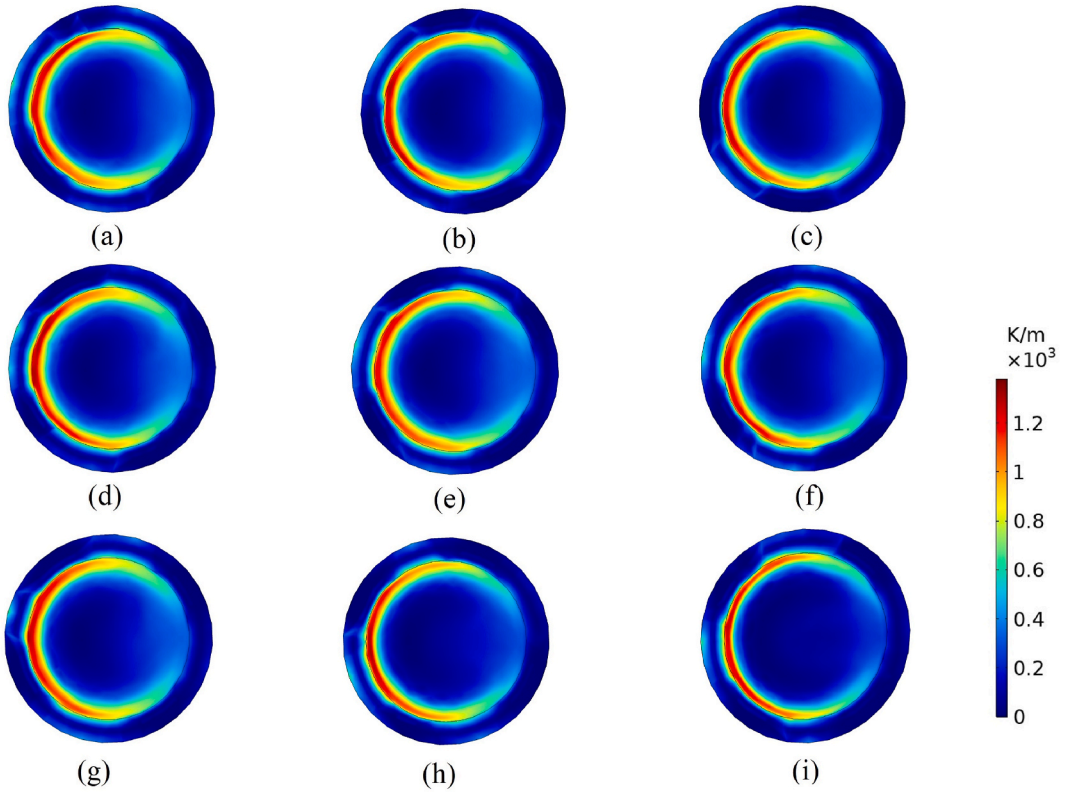

Fig. 8. The temperature gradient magnitude (a–c) conventional helical tube, (d–f) variable axial pitch(H_a = 3 cm), and (g–i) variable radial pitch (H_r = 2.5 cm).

$$j = \frac{1}{A}\iint_A \boldsymbol{\omega}.\, dA \tag{19}$$

$$\boldsymbol{\omega} = \nabla \times \boldsymbol{u} \tag{20}$$

In the above equations, **ω** and J are the curl of velocity, renowned as vorticity, and the average value of the vorticity component, respectively.

2.4. Validation

The mesh refinement study is arranged to ensure the results are accurate and independent of grid resolution. All meshes for validation of numerical simulations are produced with the aid of a physics-controlled mesh, and the criteria for convergence for all equations with relative tolerance less than 10^{-6} are considered. This mesh establishes a trade-off condition between the model's accuracy and computational time. Fig. 3 illustrates the grid resolution effect on pressure drop and outlet temperature. This figure shows five mesh configurations, namely: extremely fine, extra fine, finer, fine, normal, and coarse. The difference between extremely fine and extra fine configurations is less than 0.001% and 0.09% for outlet temperature and pressure drop, respectively. Thus, extra fine mesh is selected to conduct the numerical simulations in this work and the picture of mesh is presented in Fig. 4.

The accuracy of the present model is also compared to previous correlations. For this purpose, several correlations are used, and the results are presented in Figs. 5 and 6. The experimental correlation of reference [34] and theoretical correlation of reference [35] for friction factor are provided in Eq. (17) and Eq. (18), respectively. As can be seen from Fig. 5, the accuracy of the present work is in the acceptable range, and the maximum difference is up to 14.6%. In Fig. 6, the Nusselt number is also compared with obtained data from Manlapaz and Churchill [36]. The result shows that the maximum differences are up to 22% for the current model.

Mishra and Gupta [34]	$\frac{f}{f_{str}} = 1 + 0.033(\log_{10} Dn)^4$	$1<Dn<3000$	(21)
Manlapaz and Churchill [35]	$\frac{f}{f_{str}} = \left[\left(\frac{\sqrt{1+\left(\frac{35}{Dn}\right)^2} - 0.18}{\sqrt{1+\left(\frac{35}{Dn}\right)^2}}\right)^m + \frac{Dn}{88.33}\left(1+\frac{r}{3R}\right)^2\right]^{1/2}$	m = 2 $Dn<20$ m = 1 $20<Dn<40$ m=0 $Dn>40$	(22)

(continued on next page)

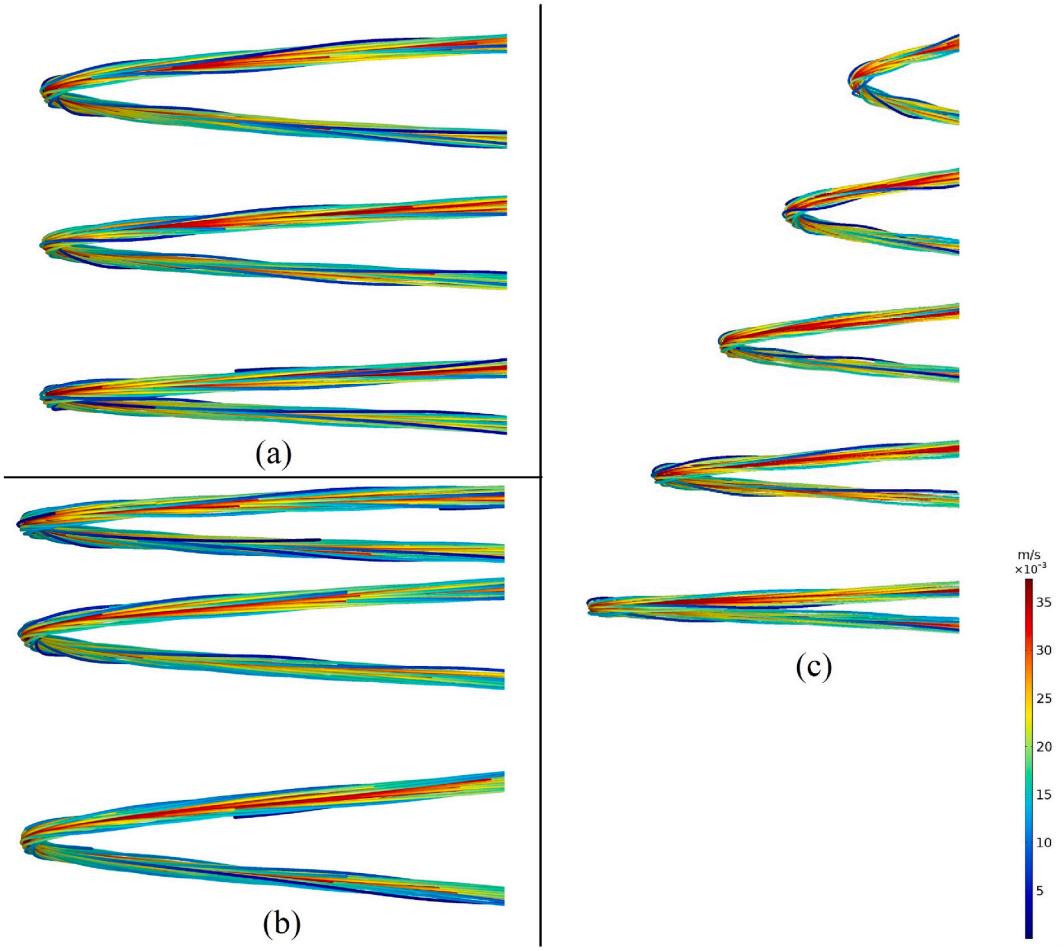

Fig. 9. The 3-D streamline for (a) conventional helical tube, (b) variable axial pitch (H_a = 3 cm), and (c) variable radial pitch (H_r = 2.5 cm).

(*continued*)

Manlapaz and Churchill [36]	$q_w = cons$	(23)
	$Nu = \left[\left(\frac{48}{11}+\frac{\frac{51}{11}}{\left(1+\frac{1342}{PrDn^2}\right)^2}\right)^3+\left(\frac{1.488\,Dn}{1+\left(\frac{1.15}{Pr}\right)}\right)^{3/2}\right]^{1/3}$	
Dean number [37]	$De = Re\sqrt{\frac{2r}{2R\left[1+\frac{P}{2\pi R}\right]^2}}$	(24)

3. Results and discussion

3.1. Flow and thermal fields

In this section, temperature and velocity profiles of the helical tubes are presented to understand the mechanism of heat transfer and fluid flow at similar working conditions. Structural parameters such as radial pitch, axial pitch, and tube diameter will likely impact the fluid flow pattern and heat transfer characteristics. A total of seven scenarios are analyzed in this paper, but three models are compared together in this section. Fig. 7 provides the velocity contours in the cross-sections of helical tubes. These plots are gathered at identical distances for three configurations and are arranged from left to right for the inlet to outlet sections. At first glance, it is evident that the maximum velocity does not appear in the centre of the tube like the velocity profile in a straight tube. This is due to the centrifugal force which pushes HTF outward of centrifugal motion. The left profiles are the nearest contours to the inlet area, the middle profiles belong to the middle of the tube, and the right contours are the closest profiles to the outlet section. The first profiles of Fig. 8(a, d, and g) for all models are almost identical, and due to the thicker boundary layer near the wall. However, velocity distribution changes by flowing the fluid in the tube. The pattern of velocity distribution in the middle of the tube for Fig. 7 (h) differs from its counterparts. The core of velocity is an oval shape, and boundary layers are relatively thinner near the solid surface. In the last

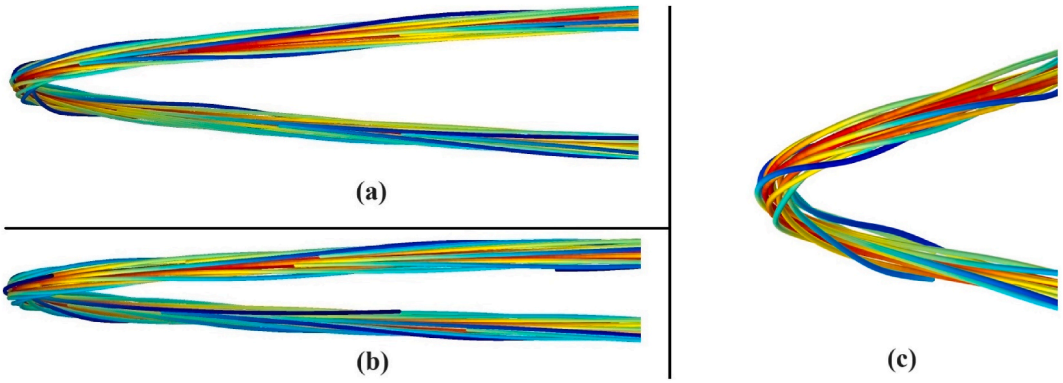

Fig. 10. The magnified 3-D streamline in the last section of the tube for (a) conventional helical tube, (b) variable axial pitch (H_a = 3 cm), and (c) variable radial pitch (H_r = 2.5 cm).

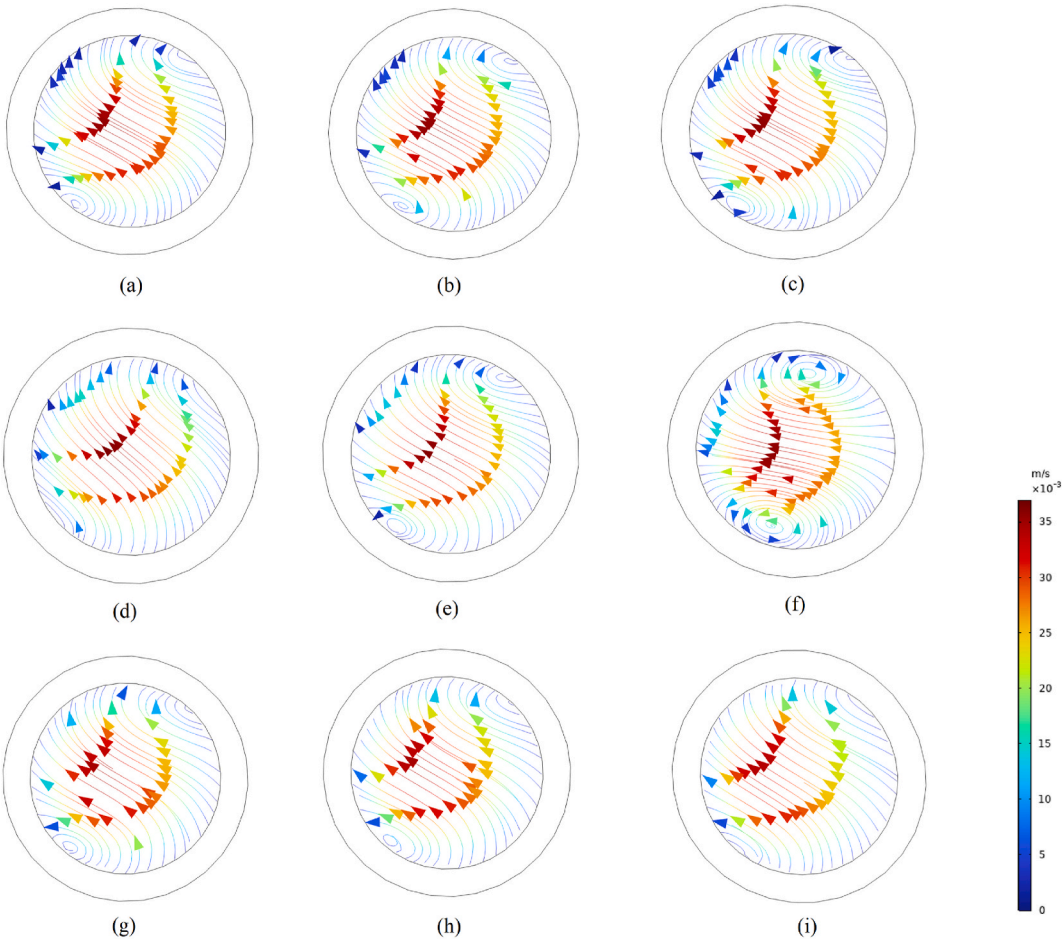

Fig. 11. The velocity counters (a–c) conventional helical tube, (d–f) variable axial pitch (H_a = 3 cm), and (g–i) variable radial pitch (H_r = 2.5 cm).

profile, the differences become more apparent. It can be seen that the variable radial pitch design in Fig. 8(i) has a velocity core like a crescent and causes a thin boundary layer near the outside of the helical tube. In contrast, for conventional and variable axial pitch designs, the velocity profile pattern almost remains constant throughout the tube. The smaller radius coil pitch at the end of the variable pitch design leads to a sharp turn of HTF and thinning of the boundary layer near the solid surface, consequently increasing the heat transfer coefficient.

Fig. 8 presents the temperature gradient magnitude of HTF to investigate the heat transfer mechanism. Like velocity profiles, these

Table 3
The vorticity magnitude along the entire flow for different cases.

Case	Re	Vorticity magnitude (1/s)					
		d = 0.7	Difference to base model %	d = 1	Difference to base model %	d = 1.3	Difference to base model %
H_r = 2.5 cm	100	7.1490	0.4439	3.5158	0.7132	2.0880	1.0355
	200	14.2770	0.5847	7.0328	0.8879	4.1905	1.2760
	400	28.1436	0.6595	13.8807	0.9997	8.3214	1.4730
	800	54.6335	0.7457	26.9846	1.1147	16.2817	1.6227
	1600	105.4454	0.8481	52.1537	1.2459	31.5405	1.7153
H_r=1.5 cm	**100**	**7.1241**	**0.0941**	**3.4965**	**0.1604**	**2.0715**	**0.2371**
	200	**14.2134**	**0.1366**	**6.9863**	**0.2209**	**4.1509**	**0.3190**
	400	**28.0031**	**0.1570**	**13.7779**	**0.2517**	**8.2350**	**0.4194**
	800	**54.3270**	**0.1805**	**26.7658**	**0.2948**	**16.1022**	**0.5024**
	1600	**104.7836**	**0.2151**	**51.6883**	**0.3424**	**31.1812**	**0.5566**
H_r = 0.5 cm	100	7.1190	0.0224	3.4917	0.0229	2.0676	0.0483
	200	14.1990	0.0352	6.9737	0.0401	4.1406	0.0700
	400	27.9707	0.0411	13.7517	0.0611	8.2092	0.1048
	800	54.2475	0.0339	26.7181	0.1161	16.0461	0.1522
	1600	104.5993	0.0389	51.5663	0.1056	31.0705	0.1996
H_a=3 cm	**100**	**7.1182**	**0.0112**	**3.4909**	**0**	**2.0667**	**0.0048**
	200	**14.1954**	**0.0098**	**6.9711**	**0.0028**	**4.1379**	**0.0048**
	400	**27.9579**	**−0.0046**	**13.7425**	**−0.0058**	**8.2006**	**0**
	800	**54.2076**	**−0.0396**	**26.6809**	**−0.0232**	**16.0185**	**−0.0199**
	1600	**104.4976**	**−0.0583**	**51.4969**	**−0.0291**	**30.9997**	**−0.0287**
H_a = 2 cm	100	7.1178	0.0056	3.4910	0.0028	2.0666	0
	200	14.1951	0.0077	6.9713	0.0057	4.1381	0.0096
	400	27.9597	0.0017	13.743	−0.0021	8.2021	0.0182
	800	54.2110	−0.0333	26.676	−0.0415	16.0252	0.0218
	1600	104.5054	−0.0508	51.4819	−0.0582	31.0151	0.0209
H_a=1 cm	**100**	**7.1183**	**0.0126**	**3.4908**	**−0.0028**	**2.0665**	**−0.0048**
	200	**14.1964**	**0.0169**	**6.9711**	**0.0028**	**4.1375**	**−0.0048**
	400	**27.9602**	**0.0035**	**13.7449**	**0.0116**	**8.2013**	**0.0085**
	800	**54.2096**	**−0.0359**	**26.6861**	**−0.0037**	**16.0260**	**0.0268**
	1600	**104.5004**	**−0.0556**	**51.5024**	**−0.0184**	**31.0216**	**0.0419**
Conventional model	100	7.1174	–	3.4909	–	2.0666	–
	200	14.1940	–	6.9709	–	4.1377	–
	400	27.9592	–	13.7433	–	8.2006	–
	800	54.2291	–	26.6871	–	16.0217	–
	1600	104.5586	–	51.5119	–	31.0086	–

contours are arranged from left to right in correspondence to fluid flow from the inlet to the outlet. The fluid gradually heats up as it flows through the tube, and due to the centrifugal force, the fluid's hotter stream appears close to the tube's outer part. The convection heat transfer coefficient rises by increasing the temperature gradient between the fluid and tube wall and by raising the boundary layer's temperature difference. For the conventional and variable axial pitch, which are illustrated in Fig. 8(a–c) and Fig. 8(d–f), this parameter almost remained unchanged from the inlet to the outlet section. However, thinning the area of high magnitude for variable design is prominent, especially near the outlet section, which is a sign of the reduced size of the thermal boundary layer. Also, as shown in Fig. 8 (i), the temperature gradient magnitude of HTF in the near wall area is higher than in other discussed models. All these conditions weaken the thermal and velocity boundary layers and raise the heat transfer coefficients for variable radial pitch design.

The 3-D streamlines are illustrated in Fig. 9 for the considered models. These profiles prove fluid particles' curvy and vortex-like path inside the helical tube. As mentioned, the fluid enters from the bottom and comes out from the top of the helical tube. The intensity of the circular movement of fluid inside the tube does not considerably change for the conventional and variable axial pitch from the inlet to the outlet area. However, the condition for variable radial pitch is different. According to Fig. 9(c), the intensity of the rotational flow is steadily promoted from the inlet to the outlet section due to reducing the helical coil radius. According to the Dean number, reducing the helical coil radius and increasing the tube diameter has a positive effect on intensifying Dean vortices, promoting fluid mixing, especially near the wall region. This leads to more chaos in the upper side of boundary layers and increases the heat transfer coefficient. To better understand the fluid flow mechanism, Fig. 10 is provided to better visualise the fluid flow pattern in the last section of the tube where fluid exits from the helical tubes.

The 2-D cross-section of the velocity vector is illustrated in Fig. 11. This figure shows the creation of Dean vortices when fluid flows inside the helical tube. While vortices are not created in every cross-section and sometimes are weak to detect from these plots, this figure proves the same level of these flow patterns inside the helical tube. Fig. 11(a–c) and 11 (d-f) show the velocity contours for conventional and variable axial pitch helical tubes. As can be seen, the weak vortices are generated near the solid wall of the tube, but the flow streams are similar in both cases. The fluid flow pattern is similar for variable radial pitch, but larger Dean vortices are created, especially near the outlet section. As mentioned, fluid mixing near the solid wall is promoted by increasing the Dean vortices; however, it is also necessary to consider this point that this is not the only reason for increasing heat transfer inside the conventional and variable pitch helical tube and other phenomenon such as thinning the boundary layer play an essential role in heat augmentation.

The vorticity magnitude of fluid flow depends on the geometry of the tube and the working condition. For a better understanding of

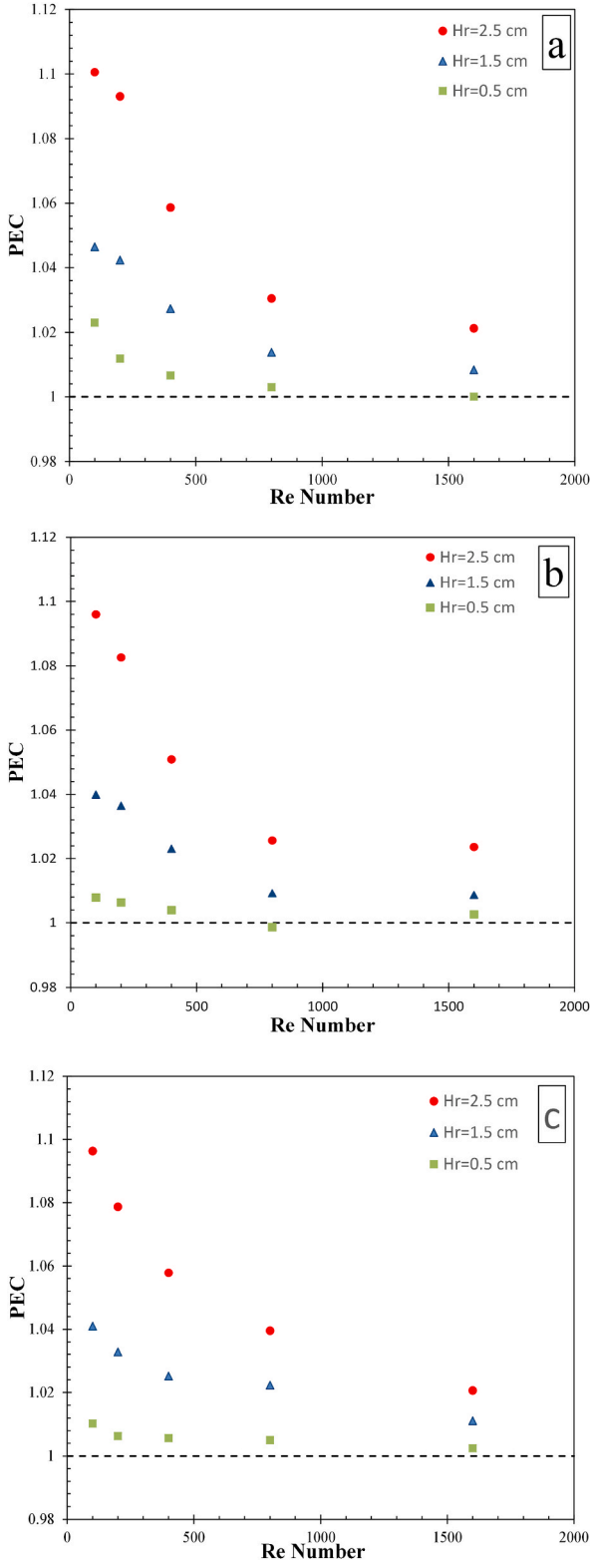

Fig. 12. The performance comparison of helical tubes with variable radius pitch (a) helical tube with d = 0.7 cm, (b) helical tube with d = 1 cm, and (c) helical tube with d = 1.3 cm.

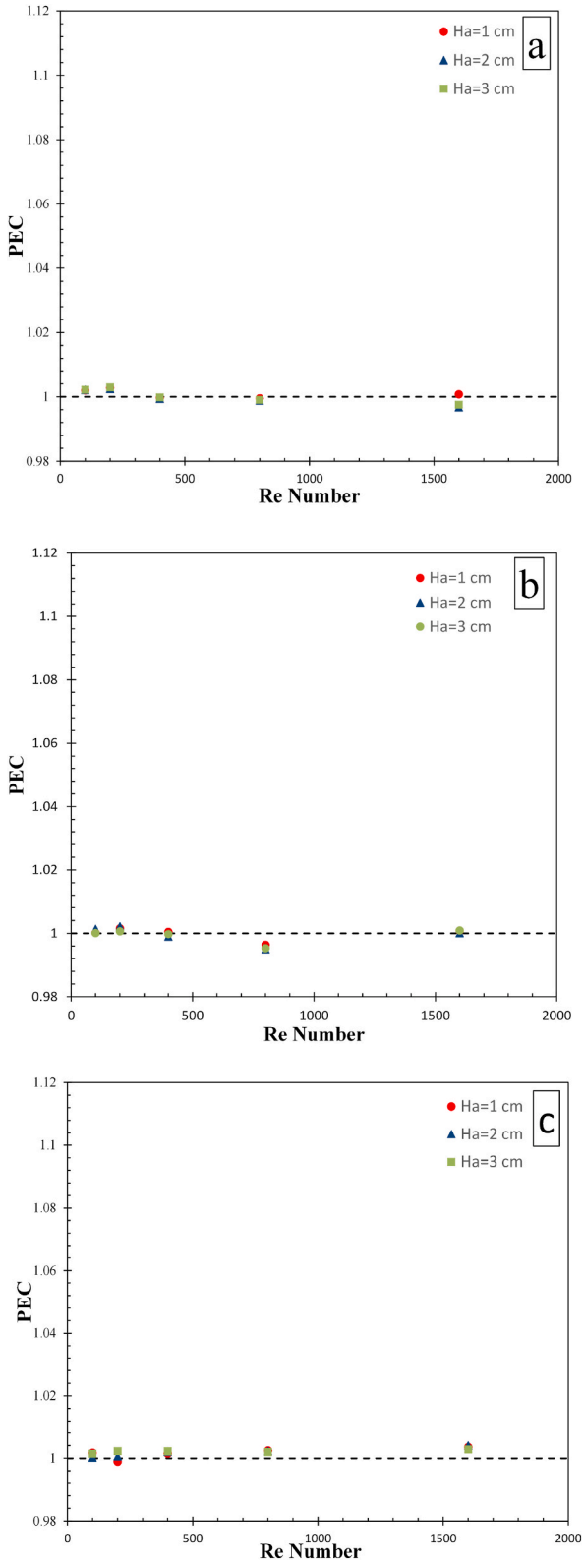

Fig. 13. The performance comparison of helical tubes with variable axial pitch (a) helical tube with d = 0.7 cm, (b) helical tube with d = 1 cm, and (c) helical tube with d = 1.3 cm.

Table 4
The thermal and fluid flow characteristics of helical tubes under different operating conditions.

Case	Re	*Nu* (average Nusselt number)			*f* (friction coefficient)			*PEC*		
		d = 0.7	d = 1	d = 1.3	d = 0.7	d = 1	d = 1.3	d = 0.7	d = 1	d = 1.3
H_r = 2.5 cm	100	5.1964	6.0326	6.5436	0.8091	0.8297	0.8421	1.1005	1.0960	1.0963
	200	7.8630	9.1291	9.7965	0.4858	0.5056	0.5194	1.0930	1.0826	1.0786
	400	11.8752	13.4999	14.7288	0.2991	0.3144	0.3238	1.0586	1.0509	1.0578
	800	16.2151	18.2655	20.9501	0.19	0.2007	0.2070	1.0304	1.0256	1.0395
	1600	20.2728	22.5209	26.5308	0.1253	0.1323	0.1391	1.0212	1.0236	1.0206
H_r=1.5 cm	**100**	**4.9177**	**5.6879**	**6.1655**	**0.7978**	**0.8140**	**0.8226**	**1.0464**	**1.0400**	**1.0410**
	200	**7.4237**	**8.6429**	**9.2696**	**0.4715**	**0.4888**	**0.5013**	**1.0422**	**1.0365**	**1.0327**
	400	**11.3709**	**12.9608**	**14.0692**	**0.2873**	**0.3016**	**0.3101**	**1.0273**	**1.0231**	**1.0251**
	800	**15.7097**	**17.6832**	**20.2359**	**0.1814**	**0.1912**	**0.1961**	**1.0138**	**1.0092**	**1.0223**
	1600	**19.7159**	**21.8304**	**25.7753**	**0.1198**	**0.1259**	**0.1312**	**1.0083**	**1.0087**	**1.0111**
H_r = 0.5 cm	100	4.8023	5.5016	5.9676	0.7951	0.8094	0.8163	1.0230	1.0078	1.0102
	200	7.1805	8.3508	8.9858	0.4663	0.4819	0.4937	1.0118	1.0063	1.0062
	400	11.0746	12.6338	13.7171	0.2821	0.2956	0.3044	1.0066	1.0039	1.0056
	800	15.4296	17.3645	19.7472	0.1775	0.1868	0.1919	1.0029	0.9986	1.0050
	1600	19.4104	21.5419	25.3487	0.1171	0.1232	0.1280	1	1.0026	1.0024
H_a=3 cm	**100**	**4.7023**	**5.4557**	**5.9101**	**0.7940**	**0.8077**	**0.8140**	**1.0021**	**1.0001**	**1.0014**
	200	**7.1081**	**8.2908**	**8.9330**	**0.4645**	**0.4796**	**0.4909**	**1.0029**	**1.0006**	**1.0022**
	400	**10.976**	**12.558**	**13.6437**	**0.2803**	**0.294**	**0.3027**	**0.9998**	**0.9997**	**1.0022**
	800	**15.3344**	**17.2748**	**19.6528**	**0.1763**	**0.1858**	**0.1909**	**0.9990**	**0.9953**	**1.0019**
	1600	**19.3176**	**21.4606**	**25.3093**	**0.1163**	**0.1225**	**0.1273**	**0.9975**	**1.0009**	**1.0028**
H_a = 2 cm	100	4.7023	5.4630	5.9029	0.7940	0.8078	0.8140	1.0021	1.0014	1.0002
	200	7.1040	8.3039	8.9188	0.4645	0.4796	0.4909	1.0023	1.0022	1.0006
	400	10.9709	12.5490	13.6410	0.2803	0.2940	0.3026	0.9993	0.9989	1.0021
	800	15.3299	17.2723	19.6536	0.1763	0.1859	0.1907	0.9988	0.9949	1.0022
	1600	19.3	21.4411	25.3387	0.1163	0.1224	0.1273	0.9967	1	1.0040
H_a=1 cm	**100**	**4.7015**	**5.4560**	**5.9116**	**0.7940**	**0.8078**	**0.8140**	**1.0019**	**1.0001**	**1.0017**
	200	**7.1065**	**8.2982**	**8.9034**	**0.4645**	**0.4796**	**0.4909**	**1.0027**	**1.0015**	**0.9989**
	400	**10.9749**	**12.5672**	**13.6305**	**0.2803**	**0.2940**	**0.3025**	**0.9996**	**1.0004**	**1.0014**
	800	**15.3414**	**17.2965**	**19.6499**	**0.1763**	**0.1859**	**0.1905**	**0.9995**	**0.9963**	**1.0024**
	1600	**19.3780**	**21.4622**	**25.3177**	**0.1163**	**0.1225**	**0.1272**	**1.0007**	**1.0008**	**1.0035**
Conventional model	100	4.6922	5.4552	5.9016	0.7940	0.8078	0.8140	–	–	–
	200	7.0866	8.2851	8.9130	0.4644	0.4795	0.4909	–	–	–
	400	10.9745	12.5587	13.6111	0.28	0.2938	0.3025	–	–	–
	800	15.3398	17.3513	19.6055	0.1760	0.1857	0.1906	–	–	–
	1600	19.3592	21.4346	25.2212	0.1162	0.1224	0.1270	–	–	–

the intensity of this parameter for different cases, Table 3 is provided. This table provides detailed information about the vorticity magnitude for different cases and the comparison to the conventional model. From this table, it is clear that Reynolds number and hydraulic diameter significantly impact vorticity magnitude. Also, it can be inferred that variable radial pitch design provides the maximum improvement in forming Dean vortices inside the helical tube.

3.2. Performance analysis of helical tubes

In the variable pitch design, the step size of each coil segment differs from adjacent sections, while the conventional design provides an identical structure in the whole part of the helical tube. In the present study, axial pitch refers to coil pitch, and radius pitch refers coil diameter, respectively. These parameters in the fluid flow direction are varied to evaluate these parameters' effect on the heat and fluid flow patterns. According to Dean's number Eq. (18), increasing the diameter of the helical tube and reducing coil diameter can improve heat transfer; however, the pressure drop should be considered as its increment would have a negative impact on the overall performance. Thus, the PEC number is introduced for evaluating overall performance enhancement. This number gives a clear view of overall performance enhancement compared to conventional design.

Fig. 12 illustrates the PEC number for evaluated cases against Reynolds numbers. As can be seen, increasing the relative pitch step leads to the augmentation of a comprehensive evaluation factor for all tube diameters. While the lowest PEC numbers are registered for the H_r = 0.5 cm case, the maximum overall performance is obtained for the helical tube with H_r = 2.5 cm. The underlying reason for this improvement is steadily reducing the coil radius in the fluid flow. The heat transfer rate decreases along the flow path by decreasing the temperature difference between the fluid and wall temperature; however, this design helps to maintain the heat transfer rate in an acceptable range by intensifying the vortex-like movement of liquid particles and thinning the boundary layers. The helical tube performance is insensitive to helical tube diameter modification, and it can be seen that the general trend for three tube diameters (d = 0.7, d = 1, and d = 1.3 cm) is identical, and this parameter has a negligible effect on the overall performance. Nearly all considered cases have a PEC number above one, which is a sign of outperforming the new designs compared to the conventional configuration. In Fig. 13, the performance of helical tubes by axial pitch modification is gathered and presented. The obtained results indicate that this method of structural modification does not significantly enhance the overall performance of helical tubes; the maximum improvement observed is under 1% for the considered models. This condition is also predictable by considering Dean's number equation. For similar structural designs, varying axial pitch has the lowest effects on promoting vortices. In terms of tube diameter, similar to a variable

radius pattern, both dimensionless parameters increase by raising the tube diameter; however, this augmentation is not high enough to outperform the basic model.

The thermal and fluid flow characteristics data of the present work is presented in Table 4. Due to the slight difference between some cases, the authors decided to provide this table to conceive better thermal and hydraulic characteristics of helical tubes. In terms of tube diameter, one can see that increasing the diameter of the tube leads to an augmentation of both the Nusselt number and friction coefficient for variable radius and axial pitches. However, this does not lead to overall performance enhancement as increasing the pressure drop hinders the outperforming of new designs, and heat transfer improvement is not high enough to precede conventional design. Working conditions significantly affect the performance, especially for variable radius pitch configurations. In lower Reynolds numbers, the heat transfer rate for these cases is higher than the base models, while the difference becomes smaller by raising the Reynolds number. This condition leads to the higher overall efficiency of variable radius designs in lower flow rates. In fact, the lower flow rates corresponding to a smaller Reynolds number lead to better results because larger heat transfer coefficients improve the PEC number for smaller pressure drops. Considering variable axial cases, increasing the Reynolds number raises the dimensionless heat transfer and decreases the friction coefficient, like the variable radius pattern. However, this increment has a non-linear and negligible impact on the PEC number. The obtained result about pitch step size also indicates that raising the radius step size improves the PEC number, and this is due to better thermal performance. In contrast, the variation of dimensionless parameters for axial step size modification is slight and inconsistent.

4. Conclusions

The new helical tube with variable pitch is introduced, and CFD simulations are carried out to study the heat transfer and fluid flow mechanism in the laminar regime ($100 \leq Re \leq 1600$). A total of 45 configurations are investigated by keeping the overall helical tube length constant to comprehend the effect of three structural parameters, axial pitch, radial pitch, and tube diameter, on the overall performance. The results verified that variable radial pitch improves the hydro-thermal performance by up to 10%, while modification of the axial pitch for different step sizes does not lead to significant improvement. Modifying tube diameter under similar working conditions reveals that this parameter has a negligible impact on the overall performance and generated velocity and temperature contours for different cases, proving that thinning the boundary layers and intensifying vortices are the primary reasons for the augmentation of overall performance in the variable radial pitch helical tube.

Author statement

Shayan Pourhemmati: Methodology, Conceptualization, Formula Verification, Software, Validation, Investigation, Data curation, Writing-original draft preparation, Writing-review & editing. Hussein A. Mohammed: Funding Acquisition, Review & editing, Formula Verification, Supervision. Abdellah Shafieian: Review & editing, Formula Verification, Supervision.

Declaration of competing interest

The authors declare that they have no known competing financial interests or personal relationships that could have appeared to influence the work reported in this paper.

Data availability

The authors are unable or have chosen not to specify which data has been used.

References

[1] Yan Cao, Hamdi Ayed, Ali E. Anqi, Omid Tutunchian, Hamed Sadighi Dizaji, Samira Pourhedayat, Helical tube-in-tube heat exchanger with corrugated inner tube and corrugated outer tube; experimental and numerical study, Int. J. Therm. Sci. 170 (2021), 107139, https://doi.org/10.1016/j.ijthermalsci.2021.107139. ISSN 1290-0729.

[2] Azim Doğuş Tuncer, Adnan Sözen, Ataollah Khanlari, Emine Yağız Gürbüz, Halil İbrahim Variyenli, Analysis of thermal performance of an improved shell and helically coiled heat exchanger, Appl. Therm. Eng. 184 (2021), 116272, https://doi.org/10.1016/j.applthermaleng.2020.116272. ISSN 1359-4311.

[3] A. Fouda, S.A. Nada, H.F. Elattar, H.A. Refaey, Abdullah S. Bin-Mahfouz, Thermal performance modeling of turbulent flow in multi tube in tube helically coiled heat exchangers, Int. J. Mech. Sci. 135 (2018) 621–638, https://doi.org/10.1016/j.ijmecsci.2017.12.015. ISSN 0020-7403.

[4] Nidal H. Abu-Hamdeh, Radi A. Alsulami, Muhyaddin J.H. Rawa, Abdulmalik A. Aljinaidi, Mashhour A. Alazwari, Mohamed A. Eltaher, Khalid H. Almitani, Khaled A. Alnefaie, Abdullah M. Abusorrah, Hatem F. Sindi, Marjan Goodarzi, Mohammad Reza Safaei, A detailed hydrothermal investigation of a helical micro double-tube heat exchanger for a wide range of helix pitch length, Case Stud. Therm. Eng. 28 (2021), 101413, https://doi.org/10.1016/j.csite.2021.101413. ISSN 2214-157X.

[5] Jinxing Wu, Songge Li, Yao Xu, Zhe Li, Jinyuan Zhao, Chunjie Xia, Yongdong Chen, Development and performance research of a helical longitudinal-groove tube with secondary flow reinforcement for heat transfer, Int. Commun. Heat Mass Tran. 137 (2022), 106265, https://doi.org/10.1016/j.icheatmasstransfer.2022.106265. ISSN 0735-1933.

[6] Yan Cao, Hamdi Ayed, Hamed Sadighi Dizaji, Mehran Hashemian, Makatar Wae-hayee, Entropic analysis of a double helical tube heat exchanger including circular depressions on both inner and outer tube, Case Stud. Therm. Eng. 26 (2021), 101053, https://doi.org/10.1016/j.csite.2021.101053. ISSN 2214-157X.

[7] E. Pavan Kumar, Anand Kumar Solanki, M. Mohan Jagadeesh Kumar, Numerical investigation of heat transfer and pressure drop characteristics in the micro-fin helically coiled tubes, Appl. Therm. Eng. 182 (2021), 116093, https://doi.org/10.1016/j.applthermaleng.2020.116093. ISSN 1359-4311.

[8] Kim.Leong Liaw, Jundika C. Kurnia, Agus P. Sasmito, Turbulent convective heat transfer in helical tube with twisted tape insert, Int. J. Heat Mass Tran. 169 (2021), 120918, https://doi.org/10.1016/j.ijheatmasstransfer.2021.120918. ISSN 0017-9310.

[9] Md. Jahid Hasan, Shams Forruque Ahmed, Arafat A. Bhuiyan, Geometrical and coil revolution effects on the performance enhancement of a helical heat exchanger using nanofluids, Case Stud. Therm. Eng. 35 (2022), 102106, https://doi.org/10.1016/j.csite.2022.102106. ISSN 2214-157X.

[10] Haiji Chen, Hazim Moria, Saba Y. Ahmed, Kottakkaran.Sooppy Nisar, Abdeliazim Mustafa Mohamed, Behzad Heidarshenas, Arsalanloo Akbar, Mohammad Mehdizadeh Youshanlouei, Thermal/exergy and economic efficiency analysis of circumferentially corrugated helical tube with constant wall temperature, Case Stud. Therm. Eng. 23 (2021), 100803, https://doi.org/10.1016/j.csite.2020.100803. ISSN 2214-157X.
[11] Safak Metin Kirkar, Alişan Gönül, Ahmet Selim Dalkilic, A sensitivity analysis of the effect of curvature ratio on the thermal-hydraulic performance in helically coiled tubes with corrugated walls, Int. J. Therm. Sci. 190 (2023), 108300, https://doi.org/10.1016/j.ijthermalsci.2023.108300. ISSN 1290-0729.
[12] Zhiqun Zheng, Xianzhen Huang, Zhiyuan Jiang, Thermal performance and heat transfer reliability analysis in helically corrugated helical tube, Int. J. Therm. Sci. 183 (2023), 107849, https://doi.org/10.1016/j.ijthermalsci.2022.107849. ISSN 1290-0729.
[13] Jundika C. Kurnia, Benitta A. Chaedir, Agus P. Sasmito, Laminar convective heat transfer in helical tube with twisted tape insert, Int. J. Heat Mass Tran. 150 (2020), 119309, https://doi.org/10.1016/j.ijheatmasstransfer.2020.119309. ISSN 0017-9310.
[14] Changgui Xie, Ibrahim B. Mansir, Ibrahim Mahariq, Pradeep Kumar Singh, Arsalanloo Akbar, Rehman Muhammad Shahzad, Fahd Jarad, Performance boost of a helical heat absorber by utilization of twisted tape turbulator, an experimental investigation, Case Stud. Therm. Eng. 36 (2022), 102240, https://doi.org/10.1016/j.csite.2022.102240. ISSN 2214-157X.
[15] Ehsan Gholamalizadeh, Ebrahim Hosseini, Mohammadreza Babaei Jamnani, Amiri Ali, Ali Dehghan saee, Ashkan Alimoradi, Study of intensification of the heat transfer in helically coiled tube heat exchangers via coiled wire inserts, Int. J. Therm. Sci. 141 (2019) 72–83, https://doi.org/10.1016/j.ijthermalsci.2019.03.029. ISSN 1290-0729.
[16] A. Fouda, S.A. Nada, H.F. Elattar, H.A. Refaey, Abdullah S. Bin-Mahfouz, Thermal performance modeling of turbulent flow in multi tube in tube helically coiled heat exchangers, Int. J. Mech. Sci. 135 (2018) 621–638, https://doi.org/10.1016/j.ijmecsci.2017.12.015. ISSN 0020-7403.
[17] H.F. Elattar, A. Fouda, S.A. Nada, H.A. Refaey, A. Al-Zahrani, Thermal and hydraulic numerical study for a novel multi tubes in tube helically coiled heat exchangers: effects of operating/geometric parameters, Int. J. Therm. Sci. 128 (2018) 70–83, https://doi.org/10.1016/j.ijthermalsci.2018.02.020. ISSN 1290-0729.
[18] Kim.Leong Liaw, Jundika C. Kurnia, Agus P. Sasmito, Laminar convective heat transfer in helical twisted multilobe tubes, Case Stud. Therm. Eng. 39 (2022), 102459, https://doi.org/10.1016/j.csite.2022.102459. ISSN 2214-157X.
[19] Xianfei Liu, Fang Wang, Zhiqiang Li, Caixia Zhu, Hui Zhang, Haofei Zhang, Parametric investigation of thermal-hydrodynamic performance in the innovative helically coiled heat exchangers in the heat pump system, Energy Build. 216 (2020), 109961, https://doi.org/10.1016/j.enbuild.2020.109961. ISSN 0378-7788.
[20] Guanghui Wang, Talib Dbouk, Dingbiao Wang, Yuanshuai Pei, Peng Xu, Honglin Yuan, Sa Xiang, Experimental and numerical investigation on hydraulic and thermal performance in the tube-side of helically coiled-twisted trilobal tube heat exchanger, Int. J. Therm. Sci. 153 (2020), 106328, https://doi.org/10.1016/j.ijthermalsci.2020.106328. ISSN 1290-0729.
[21] Taher Halawa, Andrew S. Tanious, On the use of twisting technique to enhance the performance of helically coiled heat exchangers, Int. J. Therm. Sci. 183 (2023), 107899, https://doi.org/10.1016/j.ijthermalsci.2022.107899. ISSN 1290-0729.
[22] S.W. Chang, P.-S. Wu, W.L. Cai, J.H. Liu, Turbulent flow and heat transfer of helical coils with twisted section, Appl. Therm. Eng. 180 (2020), 115919, https://doi.org/10.1016/j.applthermaleng.2020.115919. ISSN 1359-4311.
[23] M. Farnam, M. Khoshvaght-Aliabadi, M.J. Asadollahzadeh, Intensified single-phase forced convective heat transfer with helical-twisted tube in coil heat exchangers, Ann. Nucl. Energy 154 (2021), 108108, https://doi.org/10.1016/j.anucene.2020.108108. ISSN 0306-4549.
[24] Wen Luo, Huaizhi Han, Ruitian Yu, Lei Cai, Ruichen Gao, Flow and heat transfer characteristics of air and n-decane in eccentric tube-in-tube helically coiled heat exchangers, Int. J. Therm. Sci. 170 (2021), 107170, https://doi.org/10.1016/j.ijthermalsci.2021.107170. ISSN 1290-0729.
[25] Muyi Fan, Zewei Bao, Shaobei Liu, Weixing Huang, Flow and heat transfer in the eccentric annulus of the helically coiled tube-in-tube heat exchanger used in an aero-engine, Int. J. Therm. Sci. 179 (2022), 107636, https://doi.org/10.1016/j.ijthermalsci.2022.107636. ISSN 1290-0729.
[26] C.A. Nieto de Castro, S.F.Y. Li, A. Nagashima, R.D. Trengove, W.A. Wakeham, Standard reference data for the thermal conductivity of liquids, J. Phys. Chem. Ref. Data 15 (3) (1986) 1073–1086.
[27] B.E. Poling, J.M. Prausnitz, J.P. O'Connell, The Properties of Gases and Liquids, fifth ed., McGraw-Hill, 2001.
[28] C.F. Spencer, B.A. Adler, A critical review of equations for predicting saturated liquid density, J. Chem. Eng. Data 23 (1) (1978) 82–88.
[29] N.B. Vargnaftik, Tables of Thermophysical Properties of Liquids and Gases, second ed., Hemisphere Publishing, 1975.
[30] Danish Ansari, Kwang-Yong Kim, Hotspot thermal management using a microchannel-pinfin hybrid heat sink, Int. J. Therm. Sci. 134 (2018) 27–39, https://doi.org/10.1016/j.ijthermalsci.2018.07.043. ISSN 1290-0729.
[31] Wael I.A. Aly, Numerical study on turbulent heat transfer and pressure drop of nanofluid in coiled tube-in-tube heat exchangers, Energy Convers. Manag. 79 (2014) 304–316, https://doi.org/10.1016/j.enconman.2013.12.031. ISSN 0196-8904.
[32] Z.M. Lin, D.L. Sun, L.B. Wang, The relationship between absolute vorticity flux along the main flow and convection heat transfer in a tube inserting a twisted tape, Heat Mass Tran. 45 (2009) 1351–1363.
[33] L. Tang, S. Yuan, M. Malin, S. Parameswaran, Secondary vortex-based analysis of flow characteristics and pressure drop in helically coiled pipe, Adv. Mech. Eng. 9 (2017), 1687814017700059, https://doi.org/10.1177/1687814017700059, 2017.
[34] P. Mishra, S. Gupta, Momentum transfer in curved pipes. 1. Newtonian fluids, Ind. Eng. Chem. Process Des. Dev. 18 (1) (1979) 130–137, https://doi.org/10.1021/i260069a017.
[35] Romeo L. Manlapaz, Stuart W. Churchill, Fully developed laminar flow in a helically coiled tube of finite pitch, Chem. Eng. Commun. 7 (1–3) (1980) 57–78, https://doi.org/10.1080/00986448008912549.
[36] Romeo L. Manlapaz, Stuart.W. Churchill, Fully developed laminar convection from a helical coil, Chem. Eng. Commun. 9 (1–6) (1981) 185–200, https://doi.org/10.1080/00986448108911023.
[37] M. Bubolz, M. Wille, G. Langer, U. Werner, The use of dean vortices for crossflow microfiltration: basic principles and further investigation, Separation and Purification Technology 26 (1) (2002) 81–89, https://doi.org/10.1016/S1383-5866(01)00119-8. ISSN 1383-5866.